A brown fat-enriched adipokine, ASRA, is a leptin receptor antagonist that stimulates appetite

Lei Huang[1,4], Pengpeng Liu[1,2,4], Yong Du[1,4], Dongning Pan[1,5], Alexandra Lee[3], Scot A. Wolfe[1,2] and Yong-Xu Wang[1*]

[1]Department of Molecular, Cell and Cancer Biology, University of Massachusetts Chan Medical School, Worcester, MA, USA
[2]Li Weibo Institute for Rare Diseases Research, University of Massachusetts Chan Medical School, Worcester, MA, USA
[3]Program in Molecular Medicine, University of Massachusetts Chan Medical School, Worcester, MA, USA

[4]These authors contributed equally to this work: Lei Huang, Pengpeng Liu, and Yong Du

[5]Present address: Key Laboratory of Metabolism and Molecular Medicine, Department of Biochemistry and Molecular Biology, Fudan University Shanghai Medical College, Shanghai, China

*Correspondence: yongxu.wang@umassmed.edu

Abstract

The endocrine control of food intake remains incompletely understood, and whether the leptin receptor-mediated anorexigenic pathway in the hypothalamus is negatively regulated by a humoral factor is unknown. Here we identify an appetite-stimulating factor - ASRA - that acts as a leptin receptor antagonist. ASRA encodes an 8 kD protein that is abundantly and selectively expressed in adipose tissue and to a lesser extent, in liver, and is upregulated during fasting and cold. ASRA protein associates with autophagosomes and its secretion is induced by energy deficiency. Overexpression of ASRA in mice attenuates leptin receptor signaling leading to elevated blood glucose and development of severe hyperphagic obesity, whereas either adipose- or liver-specific ASRA knockout mice display increased leptin sensitivity, improved glucose homeostasis, reduced food intake, and resistance to high fat diet-induced obesity. Furthermore, ASRA is indispensable for cold-evoked feeding response. Recombinant ASRA (rASRA) protein binds to leptin receptor and suppresses leptin receptor signaling in cultured cells. In vivo, rASRA promotes food intake and increases blood glucose in a leptin receptor signaling-dependent manner. Our studies collectively show that ASRA, acting as a peripheral signal of energy deficit, stimulates appetite and regulates glucose metabolism by antagonizing leptin receptor signaling, thus revealing a previously unknown endocrine mechanism that has important implications for our understanding of leptin resistance.

Energy homeostasis is largely controlled by communications between the peripheral tissues and the central nervous system. In response to changes of the body's energy reserves and nutritional status, peptides are secreted from peripheral tissues to regulate signaling pathways in hypothalamus and brainstem, which in turn modulate food intake and body weight. Indeed, a number of peripheral anorexigenic peptides have been identified[1-5]. In contrast, very few peripheral orexigenic peptides have been identified[6, 7] and how peripheral tissues communicate with central mechanisms to stimulate appetite was less understood.

The leptin receptor signaling pathway is considered the most critical anorexigenic pathway for the control of food intake, energy balance, and body weight[8-13]. Leptin and its receptor (LepRb) exert the effects on food intake and body weight largely through activation of the Jak2-Stat3 axis in pro-opiomelanocortin (POMC)-expressing neurons and Agouti-related protein (AgRP)-expressing neurons within the arcuate nucleus (ARC) of the hypothalamus. Leptin receptor signaling also regulates glucose metabolism in POMC neurons independently of food intake and body weight[8-13]. While leptin is an effective treatment for complete or partial leptin deficiency, common forms of obesity, including diet-induced obesity, are associated with elevated endogenous leptin levels, and show an inadequate response to exogenous leptin treatment, a state characterized as leptin resistance[8-12]. Elucidating the underlying mechanisms of leptin resistance may identify regulatory pathways that can be used to modify common metabolic disorders. To date, whether peripheral tissues produce endocrine factors to attenuate leptin receptor signaling that may potentially exacerbate leptin resistance remains undefined.

Results

Identification of a brown fat (BAT)-enriched adipokine that is induced by fasting and cold

Given that leptin is selectively expressed in white fat (WAT) and that cold[14-17] and robust WAT browning[18] induce hyperphagia, we considered the possibility that a BAT-enriched adipokine might exist to counterbalance leptin signaling. We further envisioned that such an adipokine is likely upregulated during fasting. We therefore analyzed gene expression datasets[19, 20] and screened for genes that are abundantly and selectively expressed in BAT and are induced by fasting (**Extended Data Fig. 1a**). Bioinformatic tools[21, 22] were then used to predict whether any of them are potentially secreted proteins. These combined analyses led to the identification of a previously uncharacterized mouse gene 1190005I06RIK, and its human ortholog C16orf74. 1190005I06RIK gene has an open reading frame (ORF) of 111 amino acids, while C16orf74 has an ORF of 76 amino acids (**Extended Data Fig. 1b**). However, the 1190005I06RIK mRNA has an internal in-frame ATG that corresponds to

the start codon of C16orf74 and this internal ATG is flanked by a strong Kozak sequence (GACGCCATGG), raising the possibility that this represents a key translation initiation site. Indeed, two bands, 12 kD and 8 kD, were detected in HEK293 cells transfected with expression plasmids containing the mouse 111-amino acid ORF. The 8 kD band was the product of translation initiated from the internal ATG, as it disappeared when the corresponding Methionine residue was mutated to Alanine (**Extended Data Fig. 1c**). Importantly, only the 8 kD product was detected in mouse adipose tissue and adipocyte culture (**Extended Data Fig. 1d and 1e**). Thus, translation of endogenous 1190005I06RIK mRNA is initiated from the internal in-frame ATG, producing an 8 kD polypeptide with 76 amino acid residues highly homologous to human C16orf74. Neither of these proteins possesses a signal peptide, but both are predicted by SecretomeP[22] to be non-classically secreted proteins with high NN-scores that are in line with that of fibroblast growth factor 1 (Fgf1), a non-classically secreted protein. Based on its tissue expression and functional analysis described below, we named this gene as ASRA (adipose-secreted regulator of appetite). cDNA constructs encoding the 76-amino acid polypeptide were used in our studies.

ASRA was selectively expressed in adipose tissue and to a lesser extent, in liver (**Fig. 1a**). In adipose tissue, ASRA was expressed in mature adipocytes (**Extended Data Fig. 1e and 1f**). We confirmed that expression of ASRA in both adipose and liver was induced by fasting and repressed by re-feeding (**Fig. 1b**). Expression of ASRA was also upregulated by cold in these tissues (**Fig. 1c and Extended Data Fig. 1g**). Thus, ASRA expression is induced by conditions that promote a negative energy balance. In addition, liver ASRA expression was associated with high-fat diet feeding (**Fig. 1d**), while adipose ASRA expression was not significantly altered (**Extended Data Fig. 1h**).

Cultured adipocytes secreted ASRA into conditioned medium (**Extended Data Fig. 1i**). To examine ASRA secretion ex vivo, small pieces of adipose tissue were incubated with conditioned medium. While tubulin was detected in the medium in the first two hours due to initial tissue breakage, ASRA was more abundantly present at the 6-hr time point (**Fig. 1e**), indicating an active secretion. ASRA was also detected in mouse serum and human serum after enrichment with immunoprecipitation (Fig. **1f and 1g**).

ASRA associates with autophagosomes and its secretion is induced by starvation

To gain information of how ASRA is secreted, we first examined its subcellular localization. Immunofluorescent staining of endogenous ASRA in adipocytes revealed that ASRA was localized in vesicles and cell periphery (**Fig. 1h**). On the basis that autophagosome-based trafficking is one route for non-classical protein secretion[23-25] and that ASRA expression is induced by fasting, we examined

whether ASRA associates with autophagosomes. We found that some ASRA-containing vehicles were marked by the autophagosome marker LC3, and the number of these double labeled vesicles was increased under conditions of low glucose (**Fig. 1h**), indicating that ASRA vesicles evolve into or fuse with autophagosomes during energy deficiency. To further validate this observation, we expressed a fusion of GFP with the C-terminus of ASRA in adipocytes. Similar to endogenous ASRA, ASRA-GFP displayed a vesicular and cell peripheral localization pattern (**Fig. 1i**). The ASRA-GFP marked vesicles were distinct from the membrane structures of endoplasmic reticulum, Golgi and mitochondria. Instead, they almost completely overlapped with RFP-LC3 marked-autophagosomes (**Fig. 1i**). In contrast, FGF1-GFP was present in the cytoplasm and cell periphery as reported[26] (**Extended Data Fig. 1j**). Association of ASRA with autophagosomes was not cell type-specific, as similar results were also observed in COS7 cells (**Extended Data Fig. 1k**). Interestingly, low glucose medium enhanced the secretion of ASRA from adipocytes (**Fig. 1j**). We also compared ASRA-GFP and FGF1-GFP secretion in HEK293 cells by measuring GFP fluorescence intensity in medium. Secretion of ASRA-GFP was robustly increased when cells were cultured in low glucose medium, while FGF1-GFP secretion was minimally affected (**Fig. 1k**). No secretion of GFP alone was detected in either high glucose or low glucose condition. Our results indicate that ASRA secretion is mediated in part by secretory autophagosomes and is stimulated by energy deficiency.

aP2-ASRA transgenic mice are hyperphagic and severely obese

To investigate the potential in vivo function of ASRA in energy balance, we overexpressed ASRA in adipose tissue driven by the aP2 promoter. Prior to weaning (~4 weeks), there was no body weight difference between the aP2-ASRA transgenic mice and littermate controls (**Extended Data Fig. 2a**). After weaning, male aP2-ASRA mice displayed a substantial increase of body weight (**Fig. 2a**). At seven weeks, fat mass in aP2-ASRA mice was doubled and lean mass tended to increase (**Fig. 2b**). At 7 months, male aP2-ASRA mice became severely obese. They weighed 52.32 ± 0.81 g compared with 36.74 ± 1.0 g for the littermate controls, representing a 42% increase of body weight (**Fig. 2a**), which was accompanied by increased fat mass and liver steatosis (**Extended Data Fig. 2b**). Similarly, female aP2-ASRA mice had a 40% increase of body weight relative to littermate controls (**Extended Data Fig. 2c and 2d**). Interestingly, both male and female aP2-ASRA mice had a 10% increase of body length (**Fig. 2c**). Enhanced linear growth has previously been observed in hyperphagic obese mice caused by mutation within genes comprising the leptin receptor signaling pathway and downstream targets, including the leptin receptor Y1138S point mutation (which is incapable of Stat3 signaling)[27], Stat3 knockout[28], POMC knockout[29] and melanocortin-4 receptor (MC4R) knockout[30],

although the exact mechanisms are unclear. The development of obesity in aP2-ASRA mice was markedly accelerated by a high-fat diet (**Fig. 2d and Extended Data Fig. 2e**). Male aP2-ASRA mice starting on a high-fat diet at five-week-old for 11 weeks reached a body weight of 55.3 ±1.7 g (**Fig. 2d**), while wild-type mice typically need more than 20 weeks of feeding to reach a body weight of 50 g.

Prior to their development of significant obesity, we examined oxygen consumption, activity, and expression levels of genes for adipose thermogenesis and mitochondrial metabolism in regular diet-fed aP2-ASRA mice, and found no difference compared with littermate controls (**Extended Data 2f-2h**). Next, mice were individually caged at 5 weeks and food intake was measured starting at 6 weeks of age for 51 days. We found that the aP2-ASRA mice were hyperphagia, consuming, on average, 0.70 ± 0.06 g more food per day than littermate controls (**Fig. 2e**). Importantly, hyperphagia was evident at the onset of body weight divergence, as shown by the cumulative food intake at Day 2 and Day 9 (**Fig. 2e, inset**), suggesting that hyperphagia is the cause, rather than the consequence, of the obesity phenotype. To confirm this, we performed pair-feeding experiments in which the aP2-ASRA mice were offered the same amount of averaged food consumed by the control group on the previous day. Pair-fed aP2-ASRA mice had similar body weights as control mice fed ad libitum (**Extended Data Fig. 2i**), demonstrating that hyperphagia indeed underlies the obesity phenotype.

Exogenous expression of ASRA attenuates leptin receptor signaling and causes early onset of leptin resistance and elevated blood glucose

As might be expected, old aP2-ASRA mice displayed hyperleptinemia, hyperglycemia and hyperinsulinemia (**Extended Data Fig. 2j-2l**). Interestingly, in young aP2-ASRA mice, levels of circulating leptin and glucose were significantly elevated as well (**Fig. 2f and 2g**), reflecting leptin resistance. The early onset of leptin resistance promoted us to examine whether this also occurred in pair-fed aP2-ASRA mice. Indeed, these mice had increased circulating leptin and glucose levels (**Fig. 2h and 2i**), dissociating leptin resistance and elevated glucose from increased food intake and body weight. We next intraperitoneally injected vehicle or leptin into aP2-ASRA mice and littermate controls and examined Stat3 phosphorylation at Tyr705 in the hypothalamus. Basal Stat3 phosphorylation as well as leptin-induced Stat3 activation was much lower in aP2-ASRA mice (**Fig. 2j**). Fluorescent immunostaining showed that both the number and intensity of phospho-Stat3 positive neurons in the ARC of the hypothalamus were significantly decreased (**Fig. 2k**). These results together suggest that impaired leptin receptor signaling is a primary and early event in aP2-ASRA mice.

To examine the acute effect of exogenous ASRA expression on leptin receptor signaling, we tail-vein injected wild-type mice with adenoviruses expressing ASRA, which resulted in production of

ASRA protein in the liver and its secretion into circulation (**Extended Data Fig. 2m**). We found that hepatic expression of ASRA similarly increased circulating leptin and glucose levels (**Fig. 2l and 2m**). Furthermore, both basal and leptin-induced Stat3 phosphorylation in the ARC of the hypothalamus was reduced by hepatic expression of ASRA (**Fig. 2n and 2o**). These results suggest rapid and direct effects of ASRA on leptin receptor signaling and glucose homeostasis. In aggregate, exogenous expression of ASRA in peripheral tissues can both chronically and acutely attenuate hypothalamic leptin receptor signaling and thereby elevate leptin level and causes leptin resistance, which, in the aP2-ASRA mice, are largely responsible for hyperphagia, obesity and hyperglycemia.

Adipose-specific and liver-specific ASRA knockout mice have lower food intake and are resistant to high-fat diet-induced obesity (DIO)

We generated conditional ASRA mice and crossed them with Adiponectin-Cre mice to produce adipose-specific ASRA knockout (ADKO) mice (**Extended Data Fig. 3a and 3b**). We measured food intake in large cohorts. While food intake of ASRA ADKO mice in any given day often tended to be lower without statical significance, the cumulative food intake was significantly less compared with that of littermate controls (**Fig. 3a**). The lower food intake did not lead to a lower body weight (**Fig. 3b**), indicating that a compensatory response might have occurred to prevent an unsustainable energy deficit; however, expression of genes for adipose thermogenesis and mitochondrial oxidative metabolism remained unchanged (**Extended Data Fig. 3c and 3d**). We then fed male ADKO mice a high-fat diet. The ADKO mice had a more evident and persistent lower food intake (**Fig. 3c**), and as a result, these mice gained significantly less body weight and had decreased adiposity and liver weight, compared with littermate controls (**Fig. 3d and 3e, and Extended Data Fig. 3e**). Similar results were obtained in female ADKO mice on a high-fat diet (**Extended Data Fig. 3f-3h**).

Hepatic ASRA mRNA level is about 20% of that of WAT. Nonetheless, given the large liver mass, induction of hepatic ASRA expression by fasting, and the robust capacity of the liver to distribute secreted factors to other tissues[31], the physiological role of liver-secreted ASRA could be substantial. We obtained ASRA liver-specific knockout (LKO) mice (**Extended Data Fig. 3i**) by crossing ASRA conditional mice with Albumin-Cre mice. On normal chow diet, there were no significant differences in food intake and body weight between LKO mice and control mice, although LKO mice had a lower trend (**Fig. 3f and 3g**). On high-fat diet, similar to the ADKO mice, the LKO mice displayed attenuated food intake, lower body weight gain, and less fat mass and liver mass (**Fig. 3h-3j and Extended Data Fig. 3j**). Our data collectively suggest that endogenous ASRA acts as an orexigenic signal to stimulate food intake and is necessary for normal appetite, and its deficiency in either adipose or liver

consequently causes resistance to DIO. Of note, both ADKO and LKO mice maintained normal linear growth (**Extended Data Fig. 3k and 3l**).

Peripheral ASRA-deficiency sensitizes leptin action and improves glucose homeostasis

To understand the primary mechanism underlying the physiological roles of ASRA, we analyzed leptin signaling in normal chow diet-fed ASRA ADKO and LKO mice. These mice had a similar body weight as littermate controls; therefore, potential body weight and fat mass differences as confounding factors were eliminated. We found that circulating leptin level was markedly lower in the KO mice (**Fig. 4a and 4b**), especially in the ADKO mice, which had a 9-fold reduction, indicating increased leptin sensitivity. Thus, in the face of decreased ASRA level, the ASRA KO mice accordingly lowered their leptin level to avoid severe hypophagia and maintain metabolic health, underscoring a tight coordination between leptin and ASRA. Interestingly, this adjustment in leptin levels was in part mediated at the transcriptional level (**Extended Data Fig. 4a and 4b**), which was also observed in aP2-ASRA mice (**Extended Data Fig. 4c**). Lower circulating leptin level was coincided with improved glucose homeostasis (**Fig. 4c and 4d**). In further support of their leptin hypersensitivity, both basal and leptin-induced Stat3 phosphorylation in the ARC were higher in ASRA KO mice (**Fig. 4e and 4f, and Extended Data Fig. 4d and 4e**). To examine the effect of the heightened leptin sensitivity on appetite, we intraperitoneally injected a low dose of leptin (0.5 mg/kg body weight) every 12 hr and monitored food intake. While this low-dose leptin injection had little effect on food intake in control mice, as previously reported[32], it reduced food intake by 20% and 14% in ADKO and LKO mice, respectively (**Fig. 4g and 4h**). Together, our data demonstrate that peripheral ASRA-deficiency potentiates both endogenous and exogenous leptin action, revealing suppression of leptin receptor signaling as a physiological mechanism of ASRA action. SOCS3 and PTP1b are important cell-autonomous negative regulators of leptin receptor-Stat3 signaling axis. It is noteworthy that the phenotypes of ASRA KO mice largely resemble those of rodents with central deficiency of SOCS3 [33, 34] and PTP1b[32, 35], that is, increased leptin sensitivity, improved glucose homeostasis, reduced food intake and resistance to DIO.

Peripheral ASRA is required for cold-evoked feeding adaptation

Cold stimulates food intake to meet the high energy demand for heat production[14-17]. As ASRA expression is cold-induced in adipose and liver, we investigated whether ASRA is important for cold-stimulated food intake. In an 8-hr cold exposure, control mice consumed 2.07 ± 0.11 g food, more than doubled their food intake at room temperature (**Fig. 4i**). Surprisingly, the ADKO mice consumed

0.8 ± 0.08 g food, similar to their food intake at room temperature (**Fig. 4i**). Consistent with liver being increasingly appreciated as a thermogenesis-responsive organ[36], the LKO mice also had lower food intake than control mice at cold (**Fig. 4j**), which, together with the complete loss of cold-induced response in the ADKO mice, indicates that there might be a threshold of ASRA level required to enable stimulation of food intake at cold. The KO mice lost more body weight during cold exposure (**Fig. 4k and 4l**), as these mice had to metabolize stored energy to complement inadequate food intake, which was still not sufficient to maintain their core body temperature at the same level as control mice (**Fig. 4m and 4n**). Thus, peripheral ASRA has an essential role in acute cold-evoked feeding, serving as a key signal that connects thermogenesis to compensatory energy intake.

Recombinant ASRA (rASRA) protein binds to leptin receptor and directly antagonizes leptin action in cell culture

Our results presented so far strongly suggest that secreted ASRA centrally attenuates leptin receptor signaling. To further investigate its mechanism of action, we examined whether the effect of ASRA can be recapitulated in cell culture. We purified His-tagged rASRA protein from conditioned medium of Expi293F cells transfected with an ASRA expression plasmid. To aid its secretion, the N-terminus of ASRA was fused to a signal peptide. Of note, the purified rASRA protein was approximately 12 kD (**Extended Data Fig. 5a**), larger than the expected 8.6 kD, likely due to post-translational modification in the classical secretory pathway. In HEK293 cells transfected with the long form of leptin receptor, addition of leptin induced the phosphorylation of Stat3 at Tyr705 and its localization to the nucleus; this activation of Stat3 was abolished in the presence of rASRA (**Fig. 5a and 5b**). Consistent with these results, rASRA dose-dependently suppressed leptin-stimulated activity of a luciferase reporter under control of a Stat3-responsive element (**Extended Data Fig. 5b**). The effect of rASRA protein was not due to any post-translational modification, as rASRA protein purified from bacteria had a similar effect on leptin receptor signaling (**Extended Data Fig. 5c and 5d**). These results imply that the molecular target of ASRA is within the leptin receptor-Stat3 axis, with leptin receptor a likely target. To directly test this, COS7 cells transfected with vector or leptin receptor were incubated with Cy5-labeled rASRA protein. We found that association of rASRA with cell surface was dependent on the presence of leptin receptor (**Fig. 5c**). Importantly, rASRA completely colocalized with leptin receptor, suggesting that ASRA binds to leptin receptor. This binding was specific as it was largely competed away by either preincubation of unlabeled rASRA protein or leptin (**Fig. 5c**). The cytokine receptor homology domain 2 (CRH2) of leptin receptor is the major high-affinity binding site for leptin, and four consecutive hydrophobic residues (503-IFLL-506) located in CRH2 are critical for binding[37, 38]. rASRA

was not able to bind to leptin receptor when these four residues were mutated individually to Serine (**Fig. 5d, and Extended Data Fig. 5e**), indicating that ASRA and leptin likely compete for the same binding pocket. These *in vitro* results provided compelling evidence supporting a model that ASRA exerts its negative regulation on leptin receptor signaling through its interaction with leptin receptor.

rASRA protein stimulates food intake and elevates blood glucose in a leptin receptor signaling-dependent manner

ASRA was able to cross the blood-brain barrier, as rASRA injected intraperitoneally was readily detected in cerebrospinal fluid (CSF) (**Fig. 6a**). Moreover, injected Cy5-labeled rASRA bound to the ARC of the hypothalamus in a pattern that was highly overlapped with leptin receptor (**Fig. 6b**). To determine the *in vivo* effects of rASRA, we intraperitoneally injected rASRA or vehicle into individually caged wild-type lean mice and ob/ob mice and food intake was measured every 24-hr. A single dose of rASRA significantly stimulated food intake in wild-type mice (**Fig. 6c,** Day 1, p=0.0003). rASRA purified from bacteria had a similar orexigenic effect, which can be observed at the very early phase of rASRA injection (**Fig. 6d**), resembling the acute effect of Ghrelin[39] but distinct from the delayed effect of Asprosin[7]. We then injected rASRA once a day for 9 days. rASRA-treated wild-type mice continued to have a higher food consumption (**Fig. 6c**). No body weight gain was observed (**Fig. 6e**), likely due to the short-term treatment and individually-caging environment, which augments energy expenditure. Remarkably, this treatment elicited a more than 10-fold increase in leptin level (**Fig. 6f**) concomitant with an elevated glucose level (**Fig. 6g**). Thus, rASRA-treated mice mounted a compensatory response attempting to avoid overfeeding, which demonstrates both antagonism and coordination between leptin and ASRA. Despite hyperleptinemia, the rASRA-treated mice were highly leptin-resistant with a lower basal Stat3 activity in the hypothalamus (**Fig. 6h**), consistent with increased food intake. Strikingly, ob/ob mice had no response to rASRA, as neither food intake nor blood glucose was affected (**Fig. 6i and Fig. 6j**), even when they were administered a much higher dose per mouse, indicating that ASRA-stimulated food intake requires a functional leptin receptor signaling. Next, we rescued leptin signaling in ob/ob mice by injection of leptin. While exogenous leptin stimulated Stat3 phosphorylation in hypothalamus and effectively suppressed food intake in ob/ob mice as expected, these leptin-induced effects were markedly attenuated by co-injection of rASRA (**Fig. 6k and 6l**). These data provide strong *in vivo* evidence that ASRA directly antagonizes leptin receptor signaling to stimulate appetite.

Correlation of ASRA expression with human body mass index (BMI)

In a large cohort of 770 men, analysis of microarray data[40] of subcutaneous fat found that levels of ASRA were positively correlated with BMI (**Fig. 6m**). In addition, genome-wide association studies have found genetic variants of ASRA that loosely associated with type 2 diabetes in both Japanese population (rs3777457, $p=6 \times 10^{-7}$)[41] and European population (rs439967, $p=2 \times 10^{-6}$)[42]. These observations warrant future investigation of potential roles of ASRA in control of energy balance in humans.

Discussion

In this work, we identified ASRA, produced by adipose and liver, as a potent orexigenic peptide that centrally antagonizes leptin receptor signaling and regulates appetite and glucose metabolism. Intraperitoneal administration of rASRA protein causes hyperleptinemia, suppresses leptin receptor signaling and stimulates food intake. Mice with chronic overexpression of ASRA in adipose tissue are hyperphagic, severely obese, hyperleptinemic and hyperglycemic. On the other hand, ablation of ASRA in either fat or liver sensitizes leptin action, improves glucose homeostasis, reduces food intake and leads to resistance to DIO. Thus, ASRA serves as a built-in, endocrine rheostat robustly counteracting leptin receptor signaling both pharmacologically and physiologically. Remarkably, this antagonism is intrinsically coordinated with leptin, as in response to ASRA level, a feedback loop regulating leptin level, independent of body weight and adiposity, is activated to avoid excessive overfeeding or severe hypophagia. Our experimental analysis defines additional important roles of this signaling molecule in feeding response. First, peripheral ASRA is essential for acute cold-stimulated food intake, adding molecular insights into this poorly understood process. Second, ASRA associates with autophagosomes and its secretion is enhanced in response to energy deficiency, which may represent an intriguing, previously unappreciated link between peripheral cellular autophagy and hypothalamic regulation of appetite.

ASRA attenuates leptin receptor signaling by acting as a leptin receptor antagonist. This mechanistic action of ASRA distinguishes it from the other two known peripherally produced orexigenic peptides, Ghrelin and Asprosin[6, 7], which function independently of leptin receptor. There are precedents that orexigenic and anorexigenic peptides with no obvious sequence similarity can impinge upon the same receptor[5, 43]. Furthermore, in additional to the endocrine counter-regulatory mechanism we identified, the leptin receptor-Stat3 signaling axis is also negatively feedback-modulated by cell-autonomous regulators, emphasizing the need for tight control of this crucial signaling pathway by both peripheral and central regulators at different molecular levels. These

negative regulatory mechanisms may have reinforcing or complementary roles in modulating leptin receptor signaling under different physiological and pathophysiological circumstances. Adding another layer of regulation, a recent study shows that an HDAC6-regulated, adipose-secreted protein, though remains to be identified, potentiates leptin action[44].

Given the small mass of BAT, despite its enrichment of ASRA expression, the endogenous endocrine action of ASRA is conceivably attributed primarily to WAT- and liver-derived ASRA. While we currently lack a sensitive ELISA assay to reliably evaluate serum level of ASRA, ASRA mRNA expression in both adipose and liver is induced by fasting. In contrast, leptin mRNA expression in adipose[45, 46] and serum leptin level[47-49] fall during fasting. This opposing regulation in response to fasting aligns well with the action of ASRA, especially given observations that a substantial level (e.g., 20-30%) of circulating leptin is still present even after a long fasting period in rodents[47-49]. Thus, the ASRA antagonism appears to constitute a timely signaling modality to ensure sufficient feeding response, allowing a quick restore of energy balance.

Increased energy expenditure in cold elicits a compensatory hyperphagic response to maintain adiposity and body weight, and a peripheral feedback signal to the hypothalamus has been postulated[17]. Similar to fasting, ASRA expression is induced in both adipose and liver by cold, whereas leptin expression in adipose[50] and serum leptin level[49] fall. We were not able to determine whether cold induces ASRA secretion into circulation; however, it is clear that peripheral ASRA deficiency in either adipose or liver profoundly impairs cold-stimulated food intake, with the ADKO mice being completely unresponsive. Notably, aP2-Hlx transgenic mice display a robust WAT browning, and as a result, are severely hyperphagic associated with a marked increase of adipose ASRA expression[18]. Our results collectively suggest that peripheral ASRA transmits a signal of energy deficiency during fasting and cold to the hypothalamus to stimulate food intake.

At the other end of the spectrum, however, ASRA antagonism may be one of the pathogenic mechanisms underlying obesity-driven leptin resistance. Studies have suggested that leptin resistance involves an overactivation of cell-autonomous negative regulators. It would be intuitive that a humoral factor, perhaps correlated with obesity or adiposity, also plays a part. Given the expansion of adipose tissue and elevated ASRA expression in liver in DIO mice, total ASRA level is expected to markedly increase in circulation. According to our data and as would be expected for a leptin receptor antagonist, such an increase of circulating ASRA would not only exacerbate leptin resistance but also instantly elevate leptin level, which may lead to a vicious cycle in the state of obesity. We thus propose that ASRA is an important contributor to the development of leptin resistance and progression toward severe obesity. While our current study has provided important evidence

suggesting this is plausible, future investigation with temporal and simultaneous deletion of ASRA in both adipose and liver in leptin resistance-established DIO mice should further allow us to rigorously address its role.

In summary, our studies reveal a previously unknown mechanism of hormonal control of appetite in which a peripherally secreted protein ASRA serves as an antagonist of leptin receptor in the hypothalamus to attenuates leptin signaling, which may have important implications for our understanding of leptin resistance. ASRA has the potential to be a therapeutic target for obesity, diabetes, Prader-Willi syndrome, anorexia, and cancer cachexia.

1. Stanley, S., Wynne, K., McGowan, B. & Bloom, S. Hormonal regulation of food intake. *Physiological reviews* **85**, 1131-1158 (2005).
2. Coll, A.P., Farooqi, I.S. & O'Rahilly, S. The hormonal control of food intake. *Cell* **129**, 251-262 (2007).
3. Mosialou, I. *et al.* MC4R-dependent suppression of appetite by bone-derived lipocalin 2. *Nature* **543**, 385-390 (2017).
4. Williams, K.W. & Elmquist, J.K. From neuroanatomy to behavior: central integration of peripheral signals regulating feeding behavior. *Nature neuroscience* **15**, 1350-1355 (2012).
5. Ge, X. *et al.* LEAP2 Is an Endogenous Antagonist of the Ghrelin Receptor. *Cell metabolism* **27**, 461-469 e466 (2018).
6. Tschop, M., Smiley, D.L. & Heiman, M.L. Ghrelin induces adiposity in rodents. *Nature* **407**, 908-913 (2000).
7. Duerrschmid, C. *et al.* Asprosin is a centrally acting orexigenic hormone. *Nature medicine* **23**, 1444-1453 (2017).
8. Friedman, J.M. Leptin and the endocrine control of energy balance. *Nat Metab* **1**, 754-764 (2019).
9. Gautron, L. & Elmquist, J.K. Sixteen years and counting: an update on leptin in energy balance. *The Journal of clinical investigation* **121**, 2087-2093 (2011).
10. Cui, H., Lopez, M. & Rahmouni, K. The cellular and molecular bases of leptin and ghrelin resistance in obesity. *Nat Rev Endocrinol* **13**, 338-351 (2017).
11. Myers, M.G., Cowley, M.A. & Munzberg, H. Mechanisms of leptin action and leptin resistance. *Annu Rev Physiol* **70**, 537-556 (2008).
12. Wauman, J., Zabeau, L. & Tavernier, J. The Leptin Receptor Complex: Heavier Than Expected? *Frontiers in endocrinology* **8**, 30 (2017).
13. D'Souza A, M., Neumann, U.H., Glavas, M.M. & Kieffer, T.J. The glucoregulatory actions of leptin. *Mol Metab* **6**, 1052-1065 (2017).
14. Ravussin, Y., Xiao, C., Gavrilova, O. & Reitman, M.L. Effect of intermittent cold exposure on brown fat activation, obesity, and energy homeostasis in mice. *PloS one* **9**, e85876 (2014).
15. Bauwens, J.D. *et al.* Cold tolerance, cold-induced hyperphagia, and nonshivering thermogenesis are normal in alpha(1)-AMPK-/- mice. *American journal of physiology. Regulatory, integrative and comparative physiology* **301**, R473-483 (2011).
16. Bing, C. *et al.* Hyperphagia in cold-exposed rats is accompanied by decreased plasma leptin but unchanged hypothalamic NPY. *Am J Physiol* **274**, R62-68 (1998).
17. Henningsen, J.B. & Scheele, C. Brown Adipose Tissue: A Metabolic Regulator in a Hypothalamic Cross Talk? *Annu Rev Physiol* **83**, 279-301 (2021).
18. Huang, L. *et al.* Transcription factor Hlx controls a systematic switch from white to brown fat through Prdm16-mediated co-activation. *Nat Commun* **8**, 68 (2017).
19. Pan, D. *et al.* Jmjd3-Mediated H3K27me3 Dynamics Orchestrate Brown Fat Development and Regulate White Fat Plasticity. *Dev Cell* **35**, 568-583 (2015).
20. Nakai, Y. *et al.* Up-regulation of genes related to the ubiquitin-proteasome system in the brown adipose tissue of 24-h-fasted rats. *Biosci Biotechnol Biochem* **72**, 139-148 (2008).
21. Almagro Armenteros, J.J. *et al.* SignalP 5.0 improves signal peptide predictions using deep neural networks. *Nat Biotechnol* **37**, 420-423 (2019).
22. Bendtsen, J.D., Jensen, L.J., Blom, N., Von Heijne, G. & Brunak, S. Feature-based prediction of non-classical and leaderless protein secretion. *Protein Eng Des Sel* **17**, 349-356 (2004).
23. Rabouille, C. Pathways of Unconventional Protein Secretion. *Trends Cell Biol* **27**, 230-240 (2017).
24. Ponpuak, M. *et al.* Secretory autophagy. *Curr Opin Cell Biol* **35**, 106-116 (2015).
25. Claude-Taupin, A., Bissa, B., Jia, J., Gu, Y. & Deretic, V. Role of autophagy in IL-1beta export and release from cells. *Semin Cell Dev Biol* **83**, 36-41 (2018).
26. Prudovsky, I. *et al.* The intracellular translocation of the components of the fibroblast growth factor 1 release complex precedes their assembly prior to export. *J Cell Biol* **158**, 201-208 (2002).
27. Bates, S.H. *et al.* STAT3 signalling is required for leptin regulation of energy balance but not reproduction. *Nature* **421**, 856-859 (2003).
28. Piper, M.L., Unger, E.K., Myers, M.G., Jr. & Xu, A.W. Specific physiological roles for signal transducer and activator of transcription 3 in leptin receptor-expressing neurons. *Mol Endocrinol* **22**, 751-759 (2008).

29. Yaswen, L., Diehl, N., Brennan, M.B. & Hochgeschwender, U. Obesity in the mouse model of pro-opiomelanocortin deficiency responds to peripheral melanocortin. *Nature medicine* **5**, 1066-1070 (1999).
30. Huszar, D. *et al.* Targeted disruption of the melanocortin-4 receptor results in obesity in mice. *Cell* **88**, 131-141 (1997).
31. Watt, M.J., Miotto, P.M., De Nardo, W. & Montgomery, M.K. The Liver as an Endocrine Organ-Linking NAFLD and Insulin Resistance. *Endocr Rev* **40**, 1367-1393 (2019).
32. Banno, R. *et al.* PTP1B and SHP2 in POMC neurons reciprocally regulate energy balance in mice. *The Journal of clinical investigation* **120**, 720-734 (2010).
33. Kievit, P. *et al.* Enhanced leptin sensitivity and improved glucose homeostasis in mice lacking suppressor of cytokine signaling-3 in POMC-expressing cells. *Cell metabolism* **4**, 123-132 (2006).
34. Mori, H. *et al.* Socs3 deficiency in the brain elevates leptin sensitivity and confers resistance to diet-induced obesity. *Nature medicine* **10**, 739-743 (2004).
35. Picardi, P.K. *et al.* Reduction of hypothalamic protein tyrosine phosphatase improves insulin and leptin resistance in diet-induced obese rats. *Endocrinology* **149**, 3870-3880 (2008).
36. Abumrad, N.A. The Liver as a Hub in Thermogenesis. *Cell metabolism* **26**, 454-455 (2017).
37. Iserentant, H. *et al.* Mapping of the interface between leptin and the leptin receptor CRH2 domain. *Journal of cell science* **118**, 2519-2527 (2005).
38. Peelman, F., Zabeau, L., Moharana, K., Savvides, S.N. & Tavernier, J. 20 years of leptin: insights into signaling assemblies of the leptin receptor. *The Journal of endocrinology* **223**, T9-23 (2014).
39. Nakazato, M. *et al.* A role for ghrelin in the central regulation of feeding. *Nature* **409**, 194-198 (2001).
40. Civelek, M. *et al.* Genetic Regulation of Adipose Gene Expression and Cardio-Metabolic Traits. *Am J Hum Genet* **100**, 428-443 (2017).
41. Imamura, M. *et al.* Genome-wide association studies in the Japanese population identify seven novel loci for type 2 diabetes. *Nat Commun* **7**, 10531 (2016).
42. Mansour Aly, D. *et al.* Genome-wide association analyses highlight etiological differences underlying newly defined subtypes of diabetes. *Nat Genet* **53**, 1534-1542 (2021).
43. Ollmann, M.M. *et al.* Antagonism of central melanocortin receptors in vitro and in vivo by agouti-related protein. *Science* **278**, 135-138 (1997).
44. Cakir, I. *et al.* Histone deacetylase 6 inhibition restores leptin sensitivity and reduces obesity. *Nat Metab* **4**, 44-59 (2022).
45. Trayhurn, P., Thomas, M.E., Duncan, J.S. & Rayner, D.V. Effects of fasting and refeeding on ob gene expression in white adipose tissue of lean and obese (oblob) mice. *FEBS Lett* **368**, 488-490 (1995).
46. MacDougald, O.A., Hwang, C.S., Fan, H. & Lane, M.D. Regulated expression of the obese gene product (leptin) in white adipose tissue and 3T3-L1 adipocytes. *Proc Natl Acad Sci U S A* **92**, 9034-9037 (1995).
47. Ahima, R.S., Kelly, J., Elmquist, J.K. & Flier, J.S. Distinct physiologic and neuronal responses to decreased leptin and mild hyperleptinemia. *Endocrinology* **140**, 4923-4931 (1999).
48. Rayner, D.V., Simon, E., Duncan, J.S. & Trayhurn, P. Hyperleptinaemia in mice induced by administration of the tyrosine hydroxylase inhibitor alpha-methyl-p-tyrosine. *FEBS Lett* **429**, 395-398 (1998).
49. Hardie, L.J., Rayner, D.V., Holmes, S. & Trayhurn, P. Circulating leptin levels are modulated by fasting, cold exposure and insulin administration in lean but not Zucker (fa/fa) rats as measured by ELISA. *Biochem Biophys Res Commun* **223**, 660-665 (1996).
50. Puerta, M., Abelenda, M., Rocha, M. & Trayhurn, P. Effect of acute cold exposure on the expression of the adiponectin, resistin and leptin genes in rat white and brown adipose tissues. *Horm Metab Res* **34**, 629-634 (2002).

Acknowledgments

We thank the Transgenic Animal Modeling Core at University of Massachusetts Chan Medical School for the generation of ASRA transgenic mice, the Morphological Core for help on histology, and the Metabolic Core for metabolic cage studies. We thank Dr. Eric Baehrecke for providing RFP-LC3, mCherry-ER and RFP-Golgi plasmids, and Dr. Jan Tavernier for providing pXP2d2-rPAPI-luciferase plasmid. We thank Dr. Qingbo Chen for help. This work was supported by NIH R01DK116872 and R01DK115918 (to Y.-X.W.). P.P.L. and S.A.W. were supported in part by NIH 1UH3TR002668 and 1R01HL150669.

Author Contributions

L.H., P.P.L, Y.D., and D.P. designed and performed the experiments, and analyzed the data. Y.-X.W. designed the experiments and analyzed the data. S.A.W. analyzed the data. P.P.L. performed bioinformatics analysis. A.L. contributed technical assistance. L.H. and Y.-X.W. wrote the manuscript, and S.A.W. edited the manuscript.

Competing interests

Y.X.W, L.H., and Y.D. have filed a patent application on ASRA.

Methods

Identification of ASRA

Genes that are abundantly expressed in BAT (FPKM > 30), and have > 2-fold and > 10-fold expression levels in BAT relative to the levels in epididymal WAT and soleus muscle, respectively, were selected from gene expression dataset GSE56367 [19], and were further screened using dataset GSE7623 [20] for the genes within this subset that are induced by fasting. Overlapping genes from the above analyses were then predicted for secretion potential using SignalP and SecretomeP (www.cbs.dtu.dk/services)[21, 22], which resulted in the identification of 1190005I06RIK and its human orthologue C16orf74 (ASRA).

Mice

C57BL/6J wild-type mice (Stock No. 000664) and B6.Cg-*Lep*^{ob}/J (Stock No. 000632) were purchased from Jackson Laboratory. ASRA transgenic mice were generated at the core facility of UMASS Chan Medical School. Briefly, the ASRA cDNA was inserted downstream to the 5.4 kb aP2 promoter. The transgenic DNA fragment was purified using gel electrophoresis and then injected into fertilized embryos obtained from C57BL/6J×SJL hybrid mice. Transgenic lines were bred with C57BL/6J mice for a minimum of three generations. ASRA conditional knockout mice, in which exon 3 and exon 4 were flanked by two loxP sites, were generated by Biocytogen using CRISPR/Cas9 technology. The resulting floxed mice were then crossed with Adiponectin-Cre mice[51] or Alb-Cre mice[52] (Stock No. 003574, Jackson lab) to delete the last 67 amino acid residues of ASRA in adipose tissue or liver, respectively. Mice were maintained under a 12 hours light/12 hours dark cycle at 23°C with free access to food and water, unless otherwise indicated. Mice were fed either a regular diet containing 4% (w/w) fat or a high-fat diet (Bioserv, cat#S3282) containing 36% (w/w) fat. Gender-matched littermate controls were used in all experiments, and their ages were indicated accordingly. All animal studies were conducted in accordance with the guidelines approved by the Institutional Animal Care and Use Committee (IACUC) at the University of Massachusetts Medical School.

Plasmids

Mouse ASRA (76-amino acid ORF) and FGF1 cDNA were generated by PCR. ASRA-GFP and FGF1-GFP were constructed by fusing GFP to the C-terminus of ASRA or FGF1 in a mammalian expression vector. The long form of human leptin receptor (LepRb) cDNA was obtained from commercial source and point mutations were generated by PCR; all were verified by sequencing. RFP-LC3, mCherry-ER and RFP-Golgi plasmids were kindly provided by Dr. Eric Baehrecke's

laboratory. The Stat3 luciferase reporter plasmid pXP2d2-rPAPI-luciferase[37] was kindly provided by Dr. Jan Tavernier's laboratory.

Hepatic overexpression of ASRA through adenovirus infection

Adenoviral ASRA overexpression plasmid was generated using the AdEasy-1 system[53]. The plasmid was transfected into the AD-293 cells and the adenoviruses were purified through cesium chloride ultracentrifugation. The viral titers were determined by counting GFP-positive HEK293 cells infected with the viruses. Wild-type mice were tail-vein infused with GFP or ASRA adenoviruses at 1×10^{10} moi/mouse. One week after infection, serum and hypothalamuses were collected.

Expression and purification of recombinant ASRA (rASRA) protein

To aid the purification of secreted ASRA, ASRA cDNA was cloned into vector pHL-sec vector (Addgene)[54] to add a signal peptide at the N-terminus of ASRA and a 6xHis tag at its C-terminus. The ASRA expression plasmid, after removal of endotoxin, was transiently transfected into mammalian Expi293F cells (cat#A14527, ThermoFisher) cultured in suspension. Medium was collected, loaded onto a Ni-NTA Affinity column, and washed with Ni-NTA Binding/Wash Buffer (1mM TCEP, 20 mM TRIS (pH 7.5), 40 mM Imidazole, 1000 mM NaCl). rASRA protein was eluted with Elution buffer (8% Glycerol (% V/V), 1mM TCEP, 20mM TRIS (pH 7.5), 500 mM Imidazole, 500 mM NaCl). rASRA was then concentrated and buffer-exchanged into PBS via an Amicon Ultra-15 Centrifugal Filter with a 3 kDa cut-off (cat#UFC900324, Millipore). rASRA was subjected to sterile filtration utilizing a COSTAR 0.22 μm Spin-X Centrifuge Tube Filter. The concentration was measured by BCA assay. rASRA was validated with SDS-PAGE and mass spectrometry. Endotoxin level was 0.0005 EU/μg measured with a commercial kit (Thermo Scientific, #88282). rASRA protein was divided into smaller portions and stored at -80°C, with a maximum of three freeze-thaw cycles.

To purify rASRA from bacteria, ASRA cDNA with a 6xHis tag was cloned into the pET23b vector. The ASRA bacterial expression plasmid was then transformed into BL21 (DE3) cells. rASRA protein production was induced by addition of 0.5 mM IPTG, followed by an overnight incubation at 18°C. Following cell lysis, cleared cell extracts were loaded onto a Ni-NTA Affinity column, extensively washed, and eluted. rASRA protein was then concentrated and buffer-exchanged into 20 mM Tris-HCl and 150 mM NaCl. Any residual endotoxin was removed using the Pierce High Capacity Endotoxin Removal Spin Column (cat#88274, ThermoFisher). The endotoxin level was 0.001 EU/μg.

Food intake

The mice were individually housed for at least three days with ad libitum access to either a regular chow or high-fat diet prior to commencing the food intake measurements. Food intake was measured daily or at indicated time intervals. To examine the effect of leptin on food intake, ASRA knockout mice and littermate controls were intraperitoneally (ip) injected with leptin at 0.5 μg/g body weight twice a day (at 8 am and 8 pm). To measure cold-invoked feeding, ASRA knockout mice and littermate controls were housed in 4°C cold room for 8 hr from 9 am to 5 pm. To perform pair-feeding experiments, mice were housed individually for a period of 5 days, during which they had unrestricted access to regular chow. Subsequently, the aP2-ASRA mice were provided with an amount of food equivalent to the average consumption of wild type mice over the preceding 24-hour period, and body weight was monitored.

***In vivo* administration of rASRA protein**

rASRA protein purified from Expi293F cells was ip injected into wild-type mice or ob/ob mice at 65 μg/mouse or 100 μg/mouse per day, respectively. Leptin at 2 μg/g body weight per day was ip injected into ob/ob mice in co-injection experiments. In separate experiments, a single dose of rASRA protein purified from bacteria was ip injected into wild-type mice at 65 μg/g body weight. Cumulative food intake was measured at indicated time points.

Stat3 activation

To measure Stat3 activation in the hypothalamus, mice were ip injected with leptin at 1 μg/g body weight. After 45 min, mice were euthanized and hypothalamuses were obtained. Activated Stat3 (phospho-Tyr705) (cat#9145, Cell Signaling Technology) and total Stat3 (cat#9139, Cell Signaling Technology) were determined by western blot analysis. For immunofluorescence staining, hypothalamic sections that were fixed in formalin and embedded in paraffin were subjected to deparaffinization and rehydration using graded ethanol solutions. Following pre-incubation with a blocking buffer (PBS containing 5% normal goat serum and 0.3% Triton X-100) at room temperature for 60 minutes, the slides were incubated overnight at 4°C with a 1:100 dilution of phospho-Stat3-Tyr705 antibody (cat#9145, Cell Signaling Technology) in blocking buffer. Subsequently, the slides were washed and incubated with Alexa Fluor 488-conjugated secondary antibody (cat#A-11008, ThermoFisher) and DAPI (cat#D9542 Sigma) at room temperature for 2 hours.

To determine Stat3 activation in cell culture, COS7 cells were transfected with vector or human leptin receptor expression plasmids using jetOPTIMUS DNA transfection reagents (cat#101000006, Illkirch, France), following the manufacturer's instructions. After a 48-hour incubation period, cells,

serum-starved for 6 hours, were pre-incubated with rASRA protein (300 nM) for 30 min and leptin (100 nM) was then added. After 30 min, COS7 cells were fixed with 3.7% formalin at 37°C for 15 minutes and then rinsed twice with PBS. The cells were then permeabilized with ice-cold 100% methanol at -20°C for 10 minutes and washed twice with PBS. Subsequently, the cells were incubated in blocking buffer (PBS containing 5% normal goat serum and 0.3% Triton X-100) at room temperature for 60 minutes. The cells were then incubated overnight at 4°C with a 1:100 dilution of phospho-Stat3-Tyr705 antibody and a 1:200 dilution of β-actin (cat#sc-47778, Santa Cruz Biotechnology) in blocking buffer. The cells were gently washed twice with PBS and incubated with Alexa Fluor 488-conjugated (cat#A-11008, ThermoFisher) and Alexa Fluor 594-conjugated secondary antibody (cat#A-11032, ThermoFisher) for 2 hours at room temperature. Finally, the cells were incubated with DAPI (cat# D9542, Sigma) at room temperature for 30 minutes. Images were captured using an inverted Nikon Eclipse Ti2 confocal microscope (Nikon Instruments/Nikon Corp) and were processed using the same settings.

ASRA and leptin receptor binding assay

rASRA protein purified from Expi293F cells was labeled with Cyanine5 maleimide (Cy5) as per the manufacturer's instructions (cat#43080, Lumiprobe). COS7 cells were transfected with either vector, human leptin receptor, or leptin receptor mutants. After a 48-hour incubation period, the cells were gently washed with PBS, and Cy5-rASRA (300 nM) was added to the cells in FBS-free medium for 30 minutes at 37°C. The cells were then gently washed twice with PBS and fixed with 3.7% formalin at 37°C for 15 minutes without permeabilization. Next, the cells were incubated in blocking buffer (PBS containing 5% normal goat serum) at room temperature for 60 minutes. The cells were then incubated overnight at 4°C with a 1:100 dilution of leptin receptor antibody (cat#PA1-053, ThermoFisher Scientific) in blocking buffer. After incubation, the cells were gently washed twice with PBS and incubated with Alexa Fluor 488-conjugated goat anti-rabbit IgG (cat#A-11008, ThermoFisher) for 2 hours at room temperature. Finally, the cells were incubated with DAPI (cat#D9542, Sigma) at room temperature for 30 minutes. Images were captured using an inverted Nikon Eclipse Ti2 confocal microscope (Nikon Instruments/Nikon Corp) and were processed using the same settings.

Measurement of circulating glucose, insulin and leptin

Glucose level was measured using a glucose meter. Commercial ELISA kits were used to measure insulin (cat#90080, CrystalChem) and leptin (cat#90030, CrystalChem) levels, which were calculated

with four-parameter logistic curve fit. In some experiments, due to large cohorts, leptin level was measured in a randomly picked subset of serum samples.

Adipocyte culture and differentiation

The immortalized brown preadipocyte cell line was previously generated[55]. On day -2 of differentiation, brown preadipocytes at 70% confluence were cultured in Dulbecco's Modified Eagle's Medium (DMEM, cat#11965-092, Gibco) supplemented with 10% fetal bovine serum (FBS, cat#S11550, Atlanta biologicals), 20 nM insulin (cat#I6634, Sigma), 1 nM 3,3′,5-triiodo-l-thyronine (cat#T0281, Sigma), 50 units/ml penicillin, and 50 mg/ml streptomycin (differentiation medium). To induce adipocyte differentiation on day 0, the cells were cultured in differentiation medium supplemented with 0.125 mM indomethacin (cat#A19910-06, Alfa Aesar), 0.5 μM dexamethasone (cat#d4902, Sigma), and 0.5 mM isobutylmethylxanthine (cat#I7018, Sigma) for 48 hours. After the induction period, the cells were returned to the differentiation medium. The primary iWAT preadipocyte culture and differentiation were described previously[18, 19]. Preadipocytes were isolated from two-week-old mice and cultured until confluence. Differentiation was initiated by culturing the confluent cells in DMEM/F12 medium (cat#11320-033, Gibco) containing 10% FBS, 850 nM insulin, 1 nM triiodothyronine, 0.5 mM isobutylmethylxanthine, 0.5 μM dexamethasone, and 0.125 mM indomethacin. After 2 days, the cells were maintained in DMEM/F12 medium supplemented with 10% FBS, 850 nM insulin, and 1 nM triiodothyronine, with the medium being changed every 2 days. On day 6, both brown and primary iWAT adipocytes were fully differentiated, and cells with at least 95% differentiation efficiency were used in experiments.

ASRA secretion

Differentiated adipocytes were cultured in serum-free DMEM medium for 6 hr. Cell extracts and conditioned medium were collected and subjected western blot analysis using an antibody against ASRA (cat#sc-163566, Santa Cruz Biotechnology, discontinued). The specificity of the antibody was validated. To examine ASRA secretion *ex vivo*, BAT tissue was cut into small pieces and incubated with serum-free DMEM medium. At indicated time points, medium was collected and replenished with fresh serum-free DMEM medium. To examine ASRA secretion in HEK293 cells, cells were transfected with ASRA-GFP, FGF1-GFP, or GFP expression vector alone. Two days after transfection, cells were cultured in either serum-free DMEM medium containing 4.5 g/L glucose or serum-free low glucose (1 g/L) DMEM medium for 6 hr. Medium was collected and GFP signal intensity was measured by a Synergy H4 Hybrid microplate reader (BioTek, Winooski, VT) using

Gen5 software. Background signal (culture medium from cells without plasmid transfection), which was similar to that of GFP medium, was subtracted.

Collection of cerebrospinal fluid (CSF)

The collection of mouse CSF was carried out following previously described methods[56]. Briefly, a glass capillary was positioned behind the mouse's head at a 30-45° angle, ensuring that the sharp end was positioned just beyond the membrane. A volume of 100-200 μL of fluid was drawn using the syringe to establish negative pressure and remove contaminants. The membrane was approached using a micromanipulator, with care taken to avoid puncturing it while sensing resistance. Subsequently, the capillary tube was tapped through the membrane using the micromanipulator, while observing under a microscope as CSF was drawn in. The collection of CSF was allowed to occur slowly. Once the desired volume was collected, the tubing's three-way valve was closed to stop the flow of CSF. The capillary was gently removed using the micromanipulator. A collection tube (1.5 mL microcentrifuge tube with 1 μL of 20x protease inhibitor) was positioned beneath the capillary's tip. Upon opening the tubing, the syringe plunger was slowly pressed to allow the CSF to flow into the collection tube. After the collection process, the CSF was briefly centrifuged (using a 5-second pulse spin at maximum speed) to facilitate mixing with the protease inhibitor. Subsequently, the CSF samples were stored at -80 °C for further analysis.

ASRA subcellular localization

To investigate endogenous ASRA localization, mature adipocytes were cultured in serum-free DMEM medium containing either 4.5 g/L or 1 g/L glucose for 6 hr. The cells were then fixed with 3.7% formalin for 15 minutes at room temperature. After fixation, permeabilization was achieved by exposing the cells to ice-cold 100% methanol at -20°C for 10 minutes, followed by washing twice with PBS. Subsequently, the cells were incubated in blocking buffer (PBS containing 5% normal goat serum and 0.3% Triton X-100) at room temperature for 60 minutes. The cells were then subjected to overnight incubation at 4°C with a 1:100 dilution of ASRA antibody (cat#HPA049367, Sigma) and a 1:500 dilution of LC3 antibody (cat#M152-3, MBL) in the blocking buffer. The ASRA antibody was validated. After incubation, cells underwent gentle PBS washing twice and were incubated with Alexa Fluor goat anti-rabbit 488-conjugated secondary antibody (cat#A-11008, ThermoFisher) and Alexa Fluor goat anti-mouse 594-conjugated secondary antibody (cat#A-11032, ThermoFisher) for 2 hours at room temperature. Finally, cells were exposed to DAPI at room temperature for 30 minutes. The

images were obtained utilizing an inverted Nikon Eclipse Ti2 confocal microscope (Nikon Instruments/Nikon Corp) and were subjected to uniform processing settings.

To investigate ASRA-GFP localization in mature adipocytes and COS7 cells, cells were co-transfected with ASRA-GFP plasmids along with mCherry-ER, RFP-Golgi, or RFP-LC3 plasmids. Following a 48-hour post-transfection period, the cells were fixed using 3.7% formalin for 15 minutes at room temperature. Subsequently, DAPI (cat#D9542, Sigma) was applied and incubated at room temperature for 30 minutes to stain the nuclei. The images were obtained and processed as described above.

Luciferase Reporter Assay

HEK293T cells were cultured in 48-well plates and were transfected with a Stat3 luciferase reporter plasmid (pXP2d2-rPAPI-luciferase) along with human leptin receptor. A vector plasmid was included to maintain the same amount of plasmid transfected in each well. Cells were then pre-treated with indicated amounts of rASRA for 60 min and 100 nM leptin was added and incubated for overnight. Luciferase activity was measured by chemiluminescence with a Synergy H4 Hybrid microplate reader (BioTek, Winooski, VT) using Gen5 software.

Gene expression

Total RNA was extracted from mature adipocytes or tissues using TRIzol reagent (Invitrogen, cat# 15596-018) following the manufacturer's instructions. An equal amount of RNA was used for reverse transcription. Quantitative real-time PCR (qRT-PCR) was performed using SYBR green fluorescent dye (cat#1725272, Bio-Rad) on an ABI7300 PCR instrument. The ribosomal 36B4 (U36) gene was used as an internal control. The relative mRNA expression levels were calculated using the $\Delta\Delta^{-Ct}$ method. Primer sequences will be provided upon request.

Bioinformatics analysis of public gene expression datasets

We analyzed microarray data (GSE7623)[20] for fasting-induced genes. We downloaded and analyzed the RNA-seq data from GSE86338 dataset[57] using DESeq2, then plotted WAT ASAR mRNA expression during room temperature and chronic cold exposure. We downloaded and analyzed the RNA-seq data from GSE88818 dataset[58] using DESeq2, and then plotted liver ASRA mRNA expression under normal chow diet and HFD. The linear regression between ASAR and BMI was analyzed on microarray data (GSE70353)[40] from subcutaneous adipose tissue samples of a cohort of 770 men using GraphPad Prism 7.

Statistical Analysis

The sample size for this study was determined based on prior experience and existing literature in the field. The investigators conducting the mouse experiments were not blinded to the genotypes. The number of biological samples (n) were provided for each figure panel. Unless otherwise specified, the data were presented as mean ± standard error of the mean (s.e.m.), and individual data points were plotted. Statistical analyses were performed using GraphPad Prism 8.0 software. Analysis between 2 groups was performed using Student's t-test. Time course analysis was done by two-way ANOVA followed by a post-hoc test using Bonferroni's method for individual time points. Statistical significance was considered when $P < 0.05$.

51. Eguchi, J. *et al.* Transcriptional control of adipose lipid handling by IRF4. *Cell Metab* **13**, 249-259 (2011).
52. Postic, C. *et al.* Dual roles for glucokinase in glucose homeostasis as determined by liver and pancreatic beta cell-specific gene knock-outs using Cre recombinase. *J Biol Chem* **274**, 305-315 (1999).
53. He, T. *et al.* A simplified system for generating recombinant adenoviruses. *Proc Natl Acad Sci U S A* **95**, 2509-2514 (1998).
54. Aricescu, A.R., Lu, W. & Jones, E.Y. A time- and cost-efficient system for high-level protein production in mammalian cells. *Acta Crystallogr D Biol Crystallogr* **62**, 1243-1250 (2006).
55. Pan, D., Fujimoto, M., Lopes, A. & Wang, Y.X. Twist-1 is a PPARdelta-inducible, negative-feedback regulator of PGC-1alpha in brown fat metabolism. *Cell* **137**, 73-86 (2009).
56. Lim, N.K. *et al.* An Improved Method for Collection of Cerebrospinal Fluid from Anesthetized Mice. *J Vis Exp* (2018).
57. Bai, Z. *et al.* Dynamic transcriptome changes during adipose tissue energy expenditure reveal critical roles for long noncoding RNA regulators. *PLoS Biol* **15**, e2002176 (2017).
58. Siersbaek, M. *et al.* High fat diet-induced changes of mouse hepatic transcription and enhancer activity can be reversed by subsequent weight loss. *Sci Rep* **7**, 40220 (2017).

Figure 1

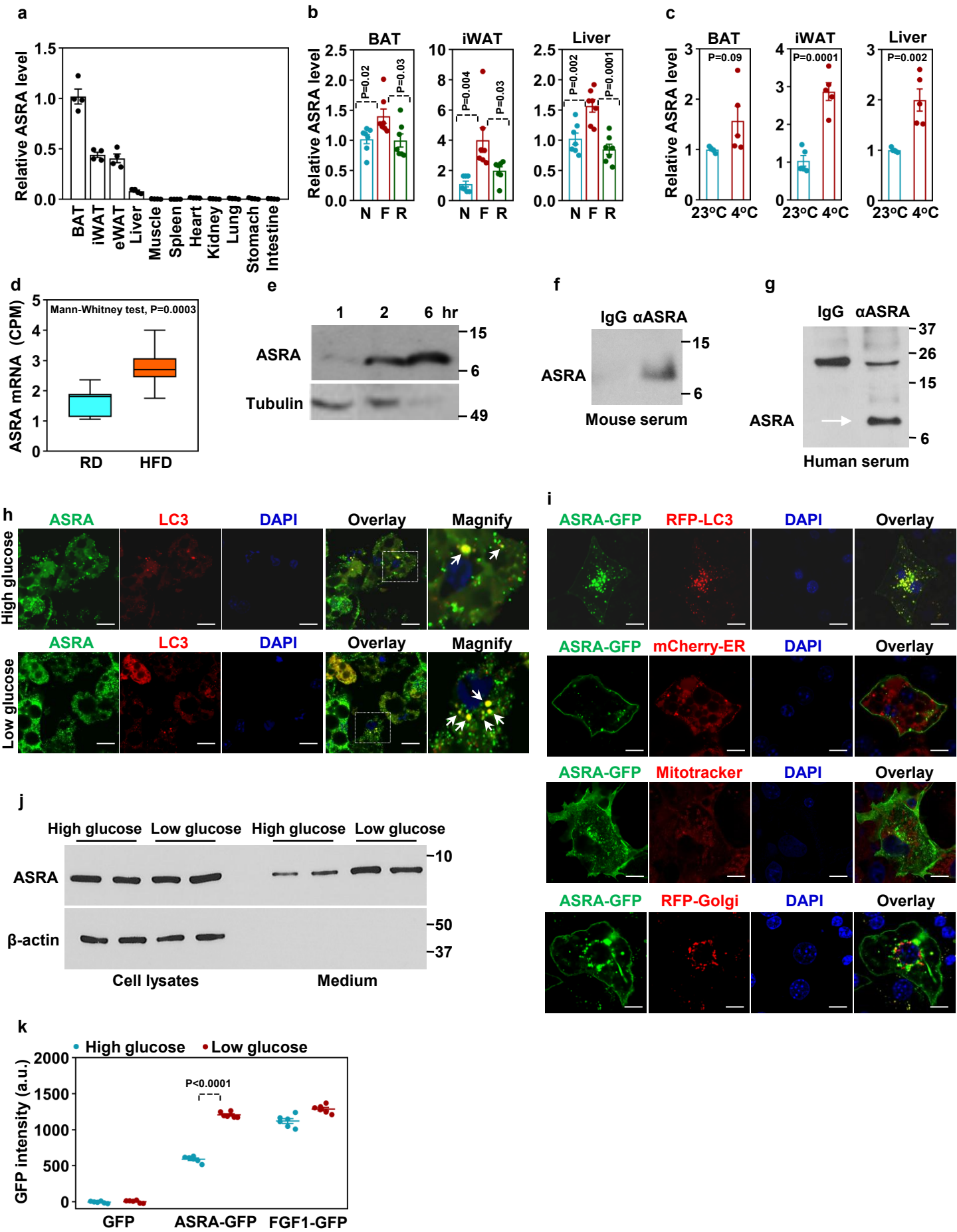
a
Relative ASRA level
BAT
iWAT
eWAT
Liver
Muscle
Spleen
Heart
Kidney
Lung
Stomach
Intestine
b
BAT
iWAT
Liver
Relative ASRA level
P=0.02
P=0.03
P=0.004
P=0.03
P=0.002
P=0.0001
N F R
c
BAT
iWAT
Liver
Relative ASRA level
P=0.09
P=0.0001
P=0.002
23°C 4°C
d
ASRA mRNA (CPM)
Mann-Whitney test, P=0.0003
RD
HFD
e
1 2 6 hr
ASRA
Tubulin
15
6
49
f
IgG αASRA
ASRA
15
6
Mouse serum
g
IgG αASRA
ASRA
37
26
15
6
Human serum
h
ASRA
LC3
DAPI
Overlay
Magnify
High glucose
Low glucose
i
ASRA-GFP
RFP-LC3
DAPI
Overlay
ASRA-GFP
mCherry-ER
DAPI
Overlay
ASRA-GFP
Mitotracker
DAPI
Overlay
ASRA-GFP
RFP-Golgi
DAPI
Overlay
j
High glucose
Low glucose
High glucose
Low glucose
ASRA
β-actin
10
50
37
Cell lysates
Medium
k
High glucose
Low glucose
GFP intensity (a.u.)
P<0.0001
GFP
ASRA-GFP
FGF1-GFP

Figure 1. Identification of ASRA as a BAT-enriched adipokine that associates with autophagosomes.

a, ASRA mRNA expression in mouse tissues (n=4). **b,** ASRA mRNA expression in BAT, iWAT, and liver of mice subjected to non-fasting (N), 12-hr fasting (F), and 3-hr re-feeding (R). n=7/group. **c,** ASRA mRNA expression in BAT, iWAT, and liver of mice subjected to 8-hr cold exposure. n=5/group. **d,** ASRA mRNA expression in liver of mice fed with regular diet (RD) (n=11) or three week high-fat diet (HFD) (n=10)[58]. **e,** ASRA secretion from BAT ex vivo. **f, g,** Detection of ASRA in mouse serum (**f**) or human serum (**g**) after immunoprecipitation with ASRA antibodies. **h,** Co-localization of endogenous ASRA and LC3 in mature adipocytes cultured in FBS-free DMEM medium containing high glucose (4.5 g/L) or low glucose (1 g/L) for 6 hr. Bar=50 μm. **i,** ASRA-GFP localization in mature adipocytes. Bar=50 μm. **j,** ASRA secretion from mature adipocytes cultured in FBS-free DMEM medium containing high glucose or low glucose for 6 hr. **k,** ASRA-GFP secretion from HEK293 cells cultured in FBS-free DMEM medium containing high glucose or low glucose for 6 hr (n=6).

Figure 2

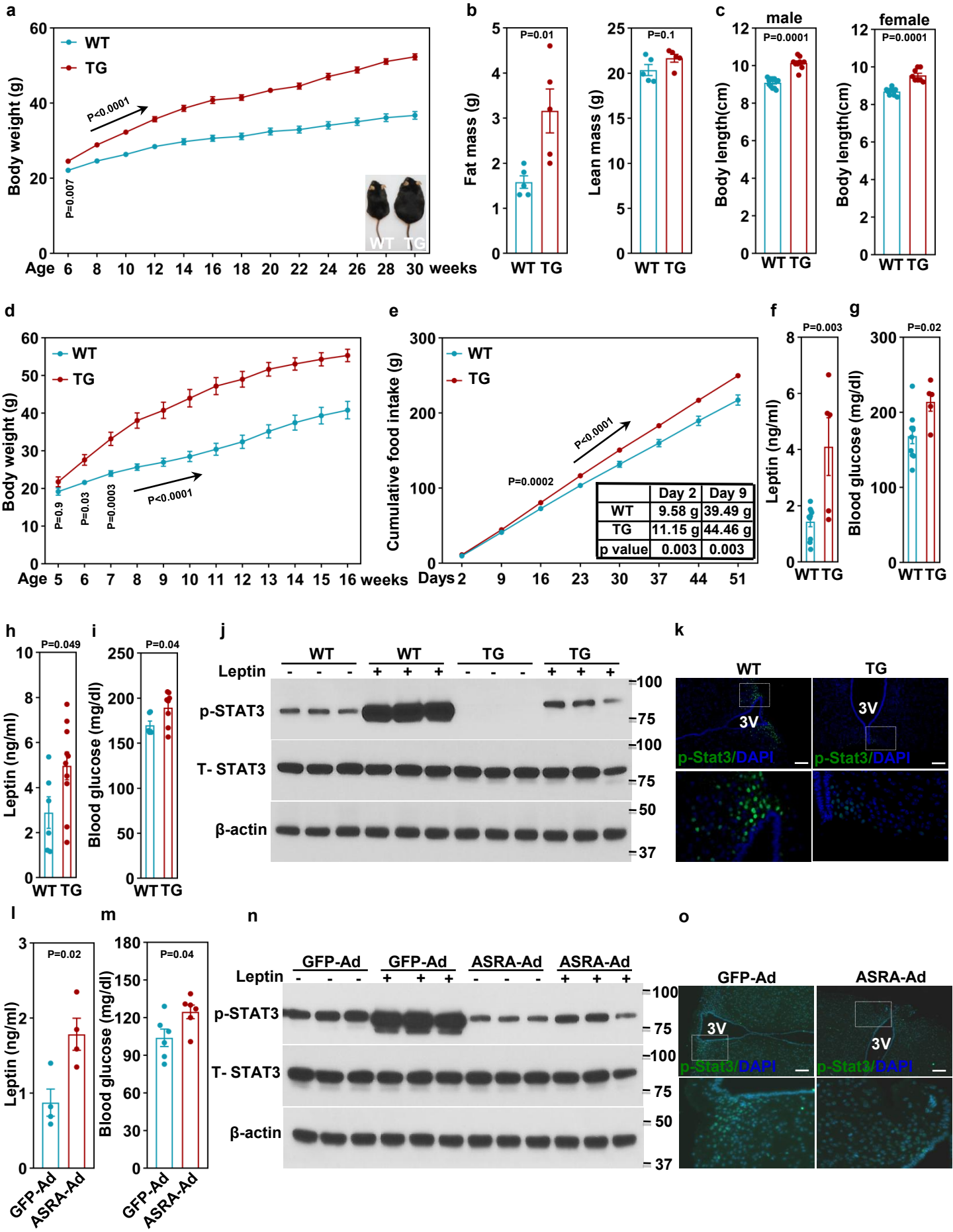
a
WT
TG
Body weight (g)
P<0.0001
P=0.007
Age 6 8 10 12 14 16 18 20 22 24 26 28 30 weeks
WT TG
b
Fat mass (g)
P=0.01
Lean mass (g)
P=0.1
WT TG
c
male
female
Body length(cm)
P=0.0001
P=0.0001
WT TG
d
Body weight (g)
P=0.9
P=0.03
P=0.0003
P<0.0001
Age 5 6 7 8 9 10 11 12 13 14 15 16 weeks
e
Cumulative food intake (g)
P<0.0001
P=0.0002
Days 2 9 16 23 30 37 44 51
Day 2 Day 9
WT 9.58 g 39.49 g
TG 11.15 g 44.46 g
p value 0.003 0.003
f
Leptin (ng/ml)
P=0.003
g
Blood glucose (mg/dl)
P=0.02
h
Leptin (ng/ml)
P=0.049
i
Blood glucose (mg/dl)
P=0.04
j
Leptin
p-STAT3
T- STAT3
β-actin
k
3V
p-Stat3/DAPI
l
Leptin (ng/ml)
P=0.02
GFP-Ad
ASRA-Ad
m
Blood glucose (mg/dl)
P=0.04
n
GFP-Ad
ASRA-Ad
o

Figure 2. Exogenous expression of ASRA attenuates leptin receptor signaling that leads to hyperphagic obesity.

a, Body weight of male aP2-ASRA (TG) mice (n=12) and littermate controls (n=13) on a chow diet. **b,** Fat mass and lean mass of ASRA TG mice (n=5) and littermate controls (n=5) at seven-week-old. **c,** Body length of male (n=9-12) and female (n=8-9) ASRA TG mice and littermate controls. **d,** Body weight of male ASRA TG mice (n=5) and littermate controls (n=7) on a high fat diet. **e,** Cumulative food intake of ASRA TG mice (n=10) and littermate controls (n=11). **f, g,** Circulating leptin (**f**) and glucose (**g**) levels in ASRA TG mice (n=5) and littermate controls (n=10) at nine-weeks-old. **h, i,** Circulating leptin (**h**) and glucose (**i**) levels in pair-fed ASRA TG mice (n=8) and ad libitum-fed littermate controls (n=6). **j,** Phosphorylation of STAT3 at Tyr705 in hypothalamus of ASRA TG mice and littermate controls that were pre-fasted for 3 hr. **k,** Phospho-STAT3 immunostaining in ASRA TG mice and littermate controls that were pre-fasted for 5 hr and then injected with leptin. Shown are representative images from 3 mice per group. Bar=200 μm. **l, m,** Circulating leptin (**l**) (n=4/group) and glucose levels (**m**) (n=6/group) of mice injected with either GFP or ASRA adenoviruses. **n,** Phosphorylation of STAT3 in mice that were pre-fasted for 3 hr. **o,** Phospho-STAT3 immunostaining in mice that were pre-fasted for 5 hr and then injected with leptin. Shown are representative images from 3 mice per group. Bar=200 μm.

Figure 3

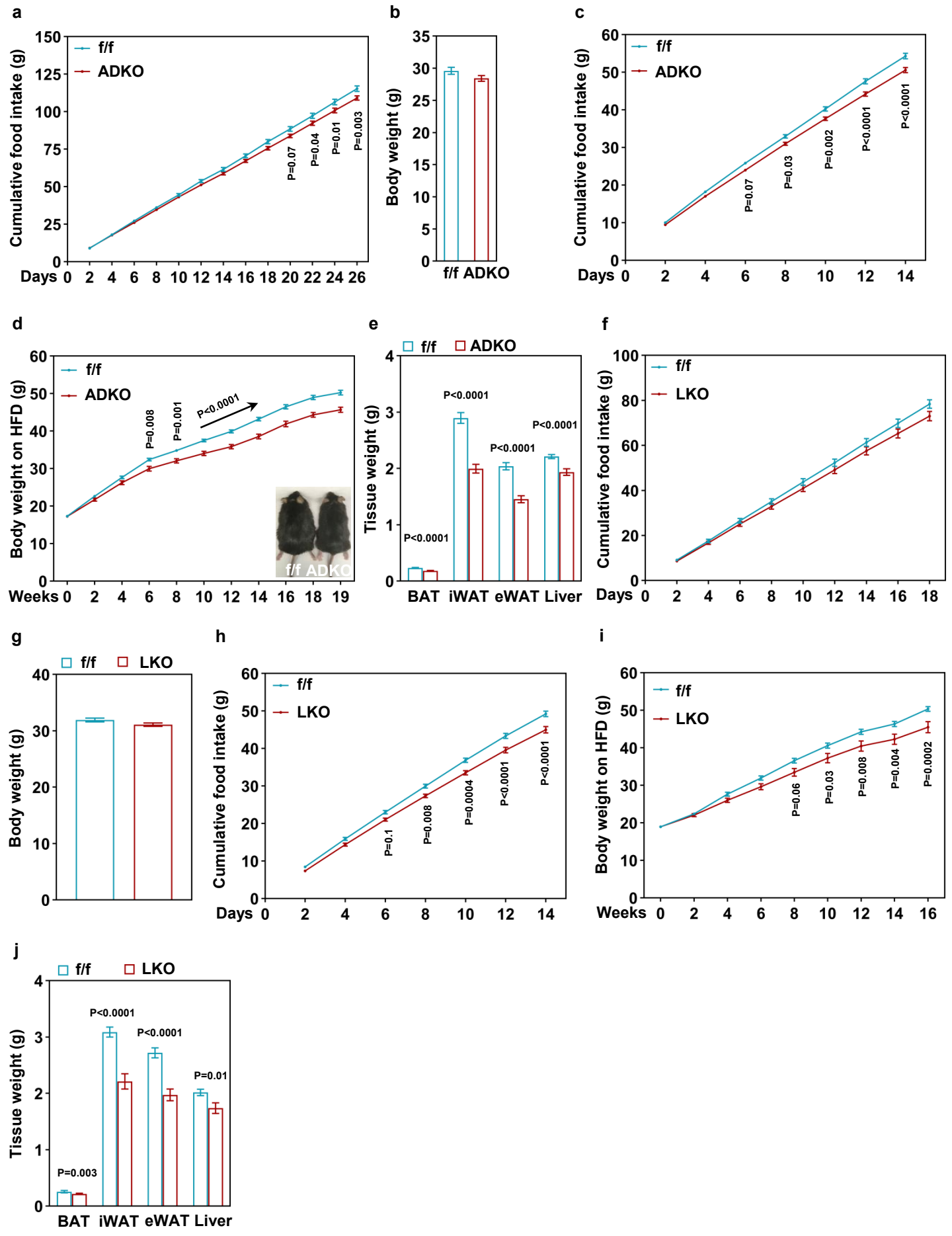
a
Cumulative food intake (g)
f/f
ADKO
P=0.07
P=0.04
P=0.01
P=0.003
Days
b
Body weight (g)
f/f ADKO
c
Cumulative food intake (g)
f/f
ADKO
P=0.07
P=0.03
P=0.002
P<0.0001
P<0.0001
Days
d
Body weight on HFD (g)
f/f
ADKO
P=0.008
P=0.001
P<0.0001
f/f ADKO
Weeks
e
f/f
ADKO
Tissue weight (g)
P<0.0001
P<0.0001
P<0.0001
P<0.0001
BAT iWAT eWAT Liver
f
Cumulative food intake (g)
f/f
LKO
Days
g
f/f
LKO
Body weight (g)
h
Cumulative food intake (g)
f/f
LKO
P=0.1
P=0.008
P=0.0004
P<0.0001
P<0.0001
Days
i
Body weight on HFD (g)
f/f
LKO
P=0.06
P=0.03
P=0.008
P=0.004
P=0.0002
Weeks
j
f/f
LKO
Tissue weight (g)
P<0.0001
P<0.0001
P=0.01
P=0.003
BAT iWAT eWAT Liver

Figure 3. Adipose-specific and liver-specific ASRA knockout mice have lower food intake and are resistant to DIO.

a, Cumulative food intake of male ASRA ADKO mice (n=37) and littermate controls (n=19) on a regular diet. **b,** Body weights of mice in (**a**) on a regular diet. n=19-37/group. **c**, Cumulative food intake of mice in (**a**) on HFD. n=19-37/group. **d,** Body weights of a second cohort of male ASRA ADKO mice (n=17) and littermate controls (n=20) on HFD. **e,** Tissue weights of mice in (**d**). n=17-20/group. **f**, Cumulative food intake of ASRA LKO mice (n=16) and littermate controls (n=16) on a regular diet. **g,** Body weights of mice in (**f**) on a regular diet. n=16/group. **h,** Cumulative food intake of mice in (**f**) on HFD. **i,** Body weights of a second cohort of male ASRA LKO mice (n=15) and littermate controls (n=18) on a HFD. **j,** Tissue weights of mice in (**i**). n=15-18/group.

Figure 4

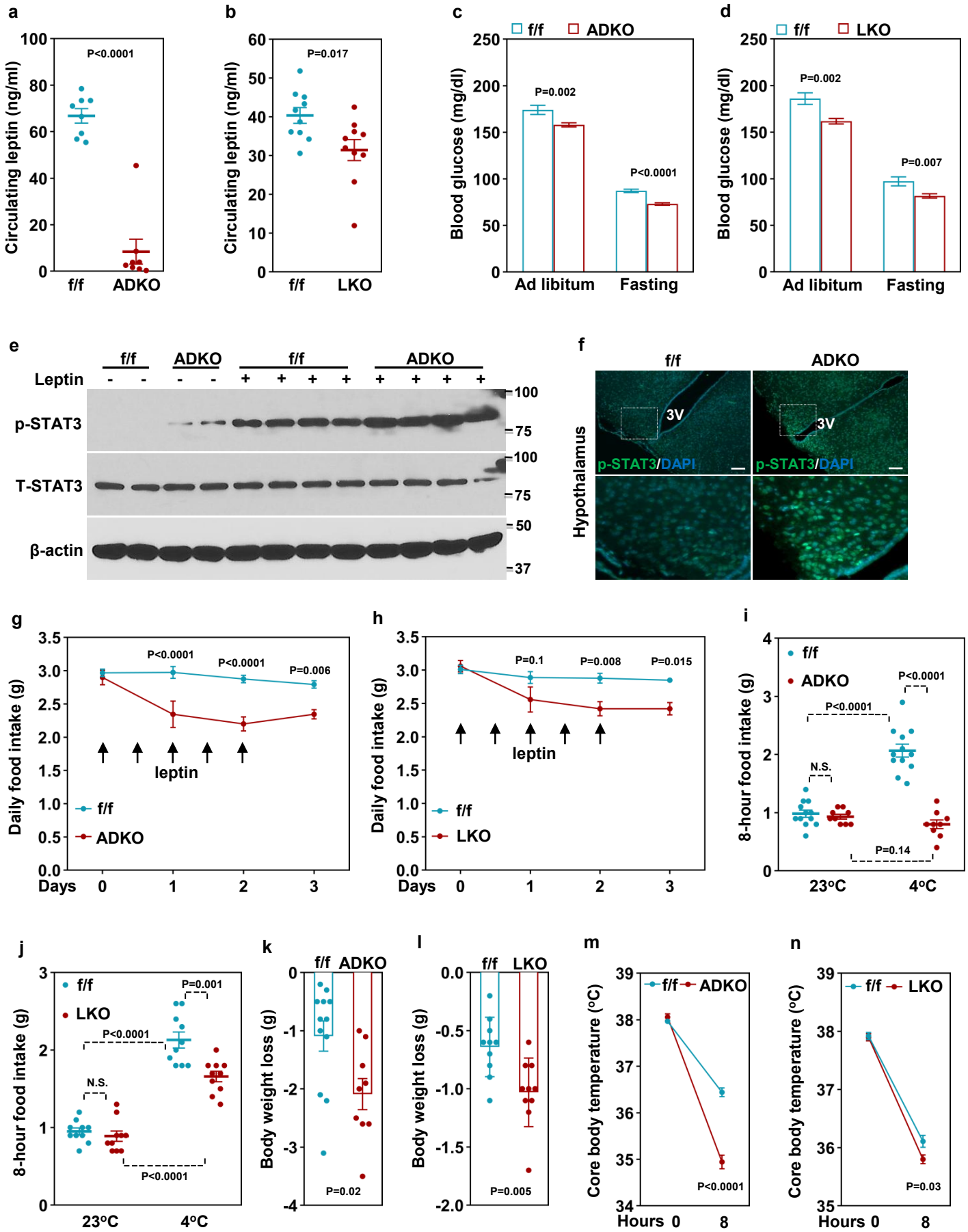
a
Circulating leptin (ng/ml)
P<0.0001
f/f
ADKO
b
Circulating leptin (ng/ml)
P=0.017
f/f
LKO
c
f/f
ADKO
Blood glucose (mg/dl)
P=0.002
P<0.0001
Ad libitum
Fasting
d
f/f
LKO
Blood glucose (mg/dl)
P=0.002
P=0.007
Ad libitum
Fasting
e
f/f
ADKO
f/f
ADKO
Leptin
p-STAT3
T-STAT3
β-actin
f
f/f
ADKO
Hypothalamus
3V
3V
p-STAT3/DAPI
p-STAT3/DAPI
g
Daily food intake (g)
P<0.0001
P<0.0001
P=0.006
leptin
f/f
ADKO
Days
h
Daily food intake (g)
P=0.1
P=0.008
P=0.015
leptin
f/f
LKO
Days
i
f/f
ADKO
8-hour food intake (g)
P<0.0001
P<0.0001
N.S.
P=0.14
23°C
4°C
j
f/f
LKO
8-hour food intake (g)
P=0.001
P<0.0001
N.S.
P<0.0001
23°C
4°C
k
f/f
ADKO
Body weight loss (g)
P=0.02
l
f/f
LKO
Body weight loss (g)
P=0.005
m
f/f
ADKO
Core body temperature (°C)
P<0.0001
Hours
n
f/f
LKO
Core body temperature (°C)
P=0.03
Hours

Figure 4. Peripheral ASRA-deficiency sensitizes leptin action and suppresses acute cold-evoked feeding.

a, Circulating leptin level in five-month-old ASRA ADKO (n=8) and control littermates (n=8). **b,** Circulating leptin level in five-month-old ASRA LKO (n=10) and littermate controls (n=10). **c,** Blood glucose of ASRA ADKO (n=37) and littermate controls (n=19) fed ad libitum or after 12-hr fasting. **d**, Blood glucose of ASRA LKO (n=16) and littermate controls (n=16) fed ad libitum or after 12-hr fasting. **e**, Phosphorylation of STAT3 in hypothalamus of mice that were pre-fasted for 3 hr. **f,** Phospho-STAT3 immunostaining in mice that were pre-fasted for 5 hr and then injected with leptin. Shown are representative images from 3 mice per group. Bar=200 μm. **g, h,** Daily food intake in male ASRA ADKO (n=9) and littermate controls (n=12) (**g**) and male LKO (n=10) and littermate controls (n=10) (**h**) that were treated with leptin (0.5 μg/g body weight) twice a day. **i, j,** Food intake in male ASRA ADKO and littermate controls (n=9-12/group) (**i**) and male LKO and littermate controls (n=10/group) during an 8-hr cold challenging. **k, l,** Body weight loss after cold challenging. **m, n,** Body temperature at 0-hr and 8-hr cold challenging.

Figure 5

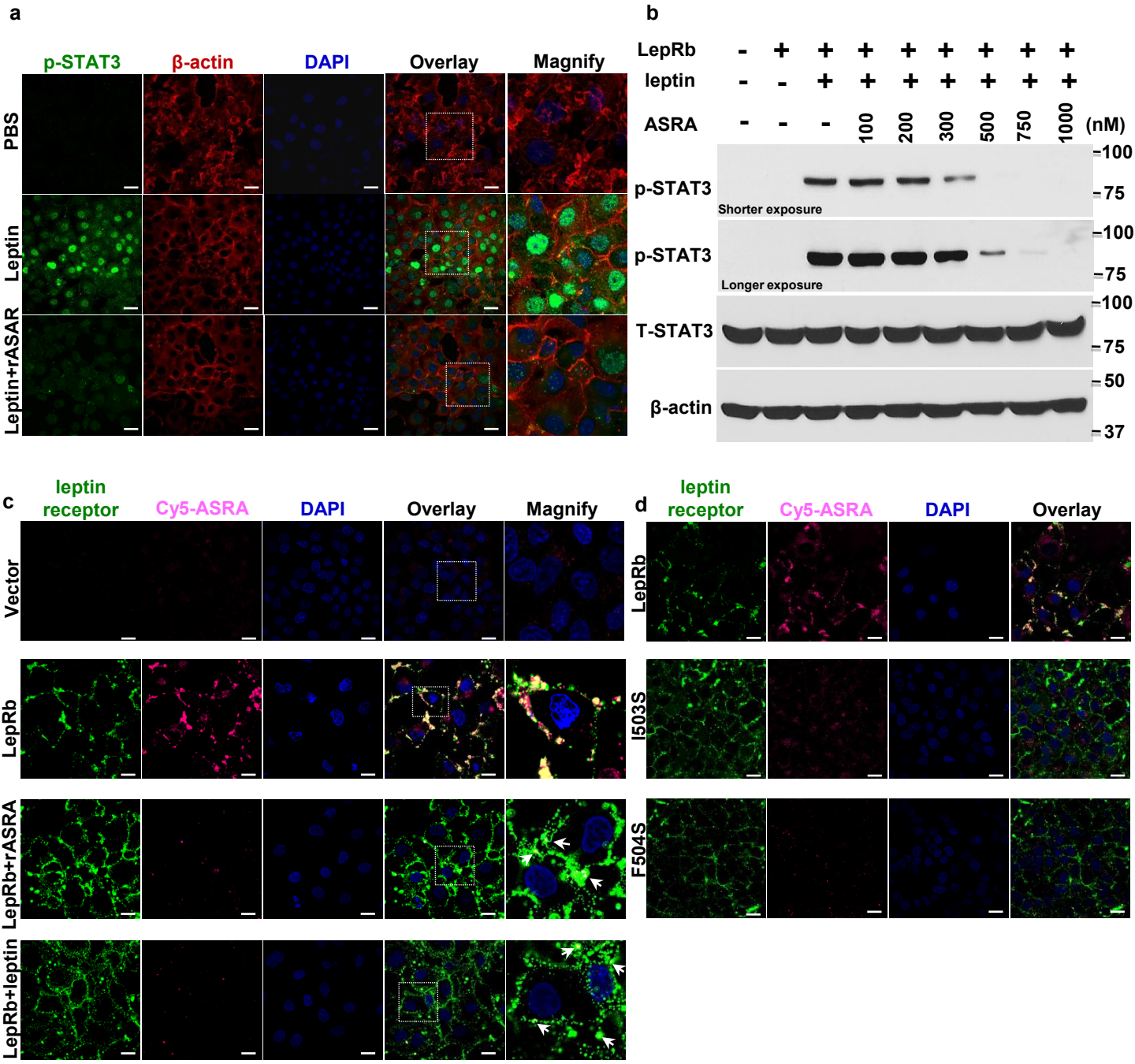
a
p-STAT3
β-actin
DAPI
Overlay
Magnify
PBS
Leptin
Leptin+rASAR
b
LepRb
leptin
ASRA
(nM)
100
200
300
500
750
1000
p-STAT3
Shorter exposure
Longer exposure
T-STAT3
β-actin
100
75
50
37
c
leptin receptor
Cy5-ASRA
DAPI
Overlay
Magnify
Vector
LepRb
LepRb+rASRA
LepRb+leptin
d
leptin receptor
Cy5-ASRA
DAPI
Overlay
LepRb
I503S
F504S

Figure 5. rASRA protein binds to leptin receptor and directly antagonize leptin action in cell culture.

a, Phospho-STAT3 immunostaining in COS7 cells transfected with the human leptin receptor. Cells were treated with rASRA (300 nM) for 30 min and leptin (100 nM) was added for another 30 min. Bar=100 μm. **b,** Western blot analysis of phospho-STAT3 of HEK293 cells treated with rASRA and leptin as described in (**a**). **c,** COS7 cells transfected with vector or the human leptin receptor (LepRb) were pre-incubated with vehicle, leptin (100 nM) or rASRA protein (300 nM) for 30 min, and then cy5-labeled rASRA protein (300 nM) was added for another 30 min. Arrows indicate remaining residual binding in the competition assays. Bar=100 μm. **d,** COS7 cells transfected with human leptin receptor or point mutations were incubated with cy5-labeled rASRA protein (300 nM) for 30 min. Bar=100 μm.

Figure 6

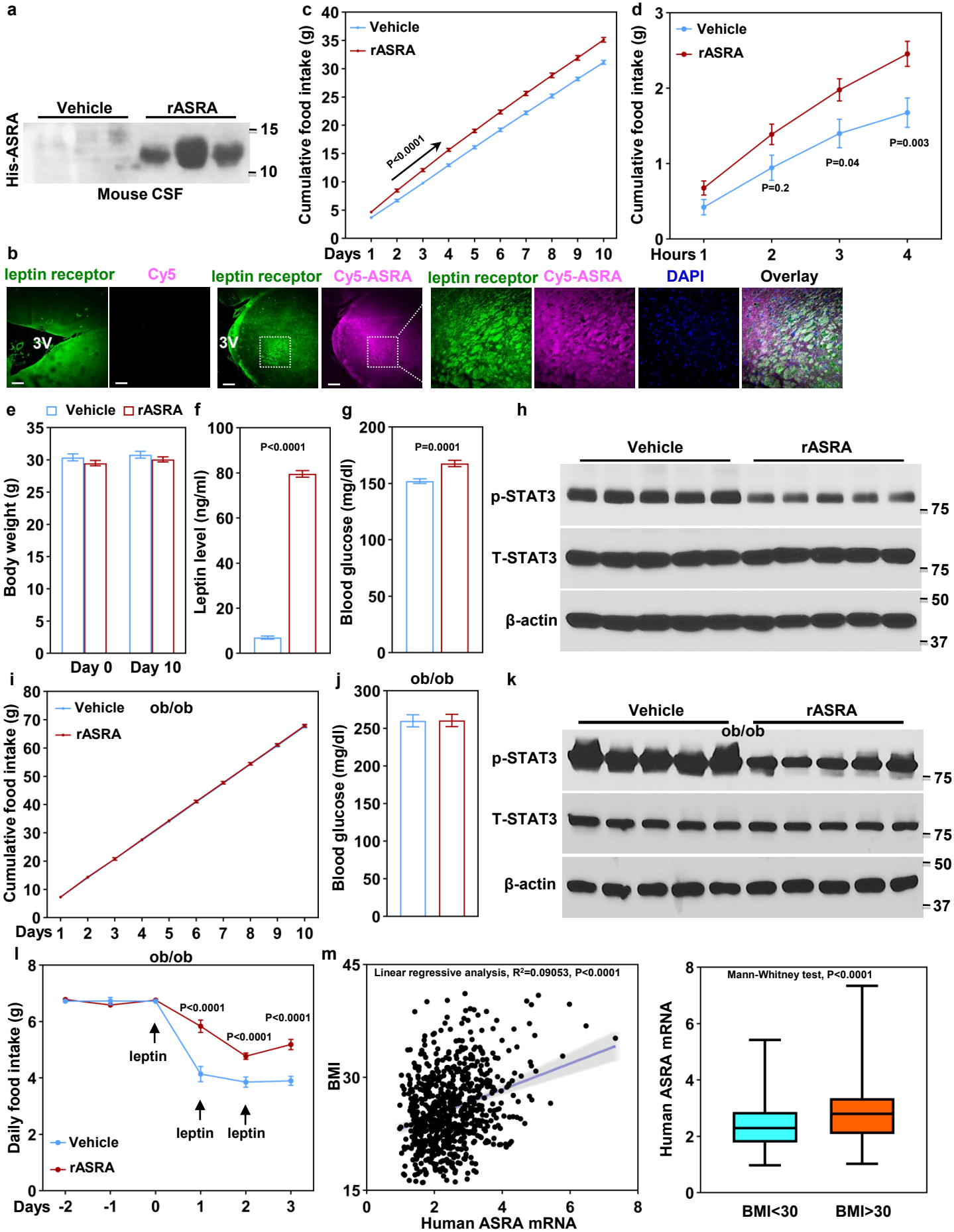
a
Vehicle
rASRA
His-ASRA
15
10
Mouse CSF
c
Vehicle
rASRA
Cumulative food intake (g)
P<0.0001
Days
d
Vehicle
rASRA
Cumulative food intake (g)
P=0.2
P=0.04
P=0.003
Hours
b
leptin receptor
Cy5
leptin receptor
Cy5-ASRA
leptin receptor
Cy5-ASRA
DAPI
Overlay
3V
3V
e
Vehicle
rASRA
Body weight (g)
Day 0
Day 10
f
Leptin level (ng/ml)
P<0.0001
g
Blood glucose (mg/dl)
P=0.0001
h
Vehicle
rASRA
p-STAT3
T-STAT3
β-actin
75
75
50
37
i
Vehicle
ob/ob
rASRA
Cumulative food intake (g)
Days
j
ob/ob
Blood glucose (mg/dl)
k
Vehicle
rASRA
ob/ob
p-STAT3
T-STAT3
β-actin
75
75
50
37
l
ob/ob
Daily food intake (g)
P<0.0001
P<0.0001
P<0.0001
leptin
leptin
leptin
Vehicle
rASRA
Days
m
Linear regressive analysis, R²=0.09053, P<0.0001
BMI
Human ASRA mRNA
Mann-Whitney test, P<0.0001
Human ASRA mRNA
BMI<30
BMI>30

Figure 6. rASRA protein induces hyperleptinemia, and stimulates food intake in a leptin receptor signaling-dependent manner.

a, Three-month-old male mice were ip injected with His-tagged rASRA protein (5.4 nmole/mouse). The presence of rASRA in CSF was detected with a His-tag antibody. **b,** Three-month-old male mice were tail-vein injected with Cy5 dye (24 nmole/mouse) or Cy5-ASRA (5.4 nmole/mouse). Two-hour post injection, the binding of Cy5-ASRA along with leptin receptor immunostaining was examined in hypothalamic slices. **c**, Three-month-old male mice were daily injected with rASRA protein (65 μg per mouse per day), and cumulative food intake was measured. n=15 per group. **d,** A single injection (65 μg) of rASRA purified from bacteria was ip injected, and cumulative food intake was measured. n=9 per group. **e,** Body weight of mice in (**c**). n=15 per group. **f,** Twelve serum samples per group at Day 10 were randomly picked up from mice in (**c**) and leptin level was measured. **g,** Blood glucose of mice in (**c**) was measured at Day 10. n=15 per group. **h,** Basal phospho-STAT3 in the hypothalamus of mice in (**c**). **i,** Three-month-old male ob/ob mice were daily injected with rASRA protein (100 μg per mouse per day), and cumulative food intake was measured. n=15. **j,** Blood glucose of mice in (**i**) was measured at Day 10. n=15 per group. **k,** Three-month-old male ob/ob mice were treated with rASRA (100 μg per mouse per day) or vehicle along with leptin (2 μg/g body weight per day) for 3 days. Phosphorylation of STAT3 in hypothalamus was examined. **l,** Daily food intake of mice in (**k**). n=15 per group. **m,** Analysis of ASRA mRNA expression in subcutaneous WAT of 770 men in relation to BMI.